AMERICAN SOCIETY FOR MICROBIOLOGY | Infection and Immunity®

BACTERIAL INFECTIONS

The Rcs Stress Response System Regulator GumB Modulates *Serratia marcescens*-Induced Inflammation and Bacterial Proliferation in a Rabbit Keratitis Model and Cytotoxicity *In Vitro*

Eric G. Romanowski,[a] Nicholas A. Stella,[a] John E. Romanowski,[a] Kathleen A. Yates,[a] Deepinder K. Dhaliwal,[a] Anthony J. St. Leger,[a] Robert M. Q. Shanks[a]

[a]Department of Ophthalmology, University of Pittsburgh School of Medicine, Pittsburgh, Pennsylvania, USA

ABSTRACT In this study, we tested the hypothesis that the conserved bacterial IgaA-family protein, GumB, mediates microbial pathogenesis associated with *Serratia marcescens* ocular infections through regulation of the Rcs stress response system. The role of the Rcs system and bacterial stress response systems for microbial keratitis is not known, and the role of IgaA proteins in mammalian pathogenesis models has only been tested with partial-function allele variants of *Salmonella*. Here, we observed that an Rcs-activated *gumB* mutant had a >50-fold reduction in proliferation compared to the wild type within rabbit corneas at 48 h and demonstrated a notable reduction in inflammation based on inflammatory signs, including the absence of hypopyons, and proinflammatory markers measured at the RNA and protein levels. The *gumB* mutant phenotypes could be complemented by wild-type *gumB* on a plasmid. We observed that bacteria with an inactivated Rcs stress response system induced high levels of ocular inflammation and restored corneal virulence to the *gumB* mutant. The high virulence of the Δ*rcsB* mutant was dependent upon the ShlA cytolysin transporter ShlB. Similar results were found for testing the cytotoxic effects of wild-type and mutant bacteria on a human corneal epithelial cell line *in vitro*. Together, these data indicate that GumB regulates virulence factor production through the Rcs system, and this overall stress response system is a key mediator of a bacterium's ability to induce vision-threatening keratitis.

KEYWORDS IgaA, Rcs system, RcsB, *Serratia marcescens*, cornea, infection, keratitis, stress response

The role for bacterial stress systems has been demonstrated as being essential for establishing wild-type (WT) levels of microbial pathogenesis in several animal models of infection (1). These include bacterial cell envelope stress response systems in both Gram-negative and Gram-positive bacteria that protect the cell envelope from external and internal host defense factors (2). The Rcs system is well studied in *Escherichia coli* and *Salmonella enterica* and conserved in other members of the order *Enterobacterales* (3). The Rcs system has a role in responding to envelope stress caused by membrane-affecting agents, including detergents and cell wall-damaging compounds such as lysozyme (3). Mutational inactivation of the Rcs system has been reported to increase the virulence potential of several bacteria, including *Proteus mirabilis* in a *Galleria mellonella* infection model (4), *Edwardsiella tarda* in a zebrafish model (5), and *S. marcescens* in a murine bacteremia model (6). Similarly, the increased virulence of *Yersinia pestis* compared to other *Yersinia* species is thought to be partially due to an incomplete Rcs system (3). In other models, Rcs system-defective mutants are less virulent. For example, *Citrobacter rodentium* and *E. coli rcsB* mutants were less virulent in rodent intestinal infection models (7, 8). Therefore, it is likely that bacteria tightly control the Rcs system during infection because it is important in regulating the expression of genes that balance host-pathogen interactions.

Citation Romanowski EG, Stella NA, Romanowski JE, Yates KA, Dhaliwal DK, St. Leger AJ, Shanks RMQ. 2021. The Rcs stress response system regulator GumB modulates *Serratia marcescens*-induced inflammation and bacterial proliferation in a rabbit keratitis model and cytotoxicity *in vitro*. Infect Immun 89: e00111-21. https://doi.org/10.1128/IAI.00111-21.

Editor Denise Monack, Stanford University

Address correspondence to Robert M. Q. Shanks, shanksrm@upmc.edu.

Received 24 February 2021
Returned for modification 17 March 2021
Accepted 23 March 2021
Accepted manuscript posted online 5 April 2021
Published 15 July 2021

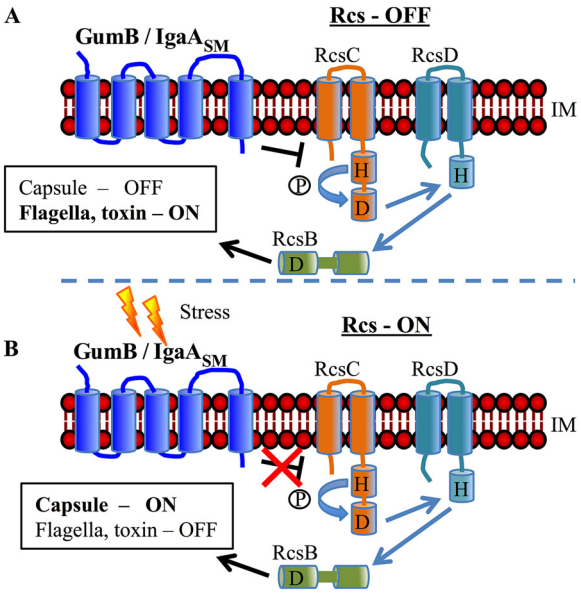

FIG 1 Model for Rcs system regulation of capsular polysaccharide and ShlA cytolysin production. (A) In the absence of Rcs-sensed stresses, GumB ($IgaA_{SM}$) inhibits the Rcs system, leading to ShlA toxin expression and very little capsule production. (B) In the presence of envelope stress, GumB no longer inhibits the Rcs system, leading to capsule biosynthesis and reduced ShlA production. Therefore, a Δ*gumB* mutant has a constitutive Rcs-ON phenotype. IM indicates inner membrane. This is a simplified model covering the factors evaluated in this study. RcsF, which transmits the stress signal to GumB and other regulators, including FliA and RcsA, is not shown. H indicates histidine; D represents aspartate; phosphate is indicated by encircled letter P.

The Rcs system is inhibited by the inner membrane protein IgaA (Fig. 1) and is essential for growth in *E. coli* and *Salmonella* species (3). The *S. marcescens* IgaA ortholog GumB is functionally conserved with other IgaA-family proteins, as *gumB* mutant defects can be complemented in *trans* by *E. coli*, *Klebsiella pneumoniae*, and *S. enterica* IgaA orthologs (9). However, unlike *E. coli* and *S. enterica*, IgaA proteins are not essential for viability in *P. mirabilis* (10) or *S. marcescens* (9). It is also likely not essential in *Y. pestis*, as it has not turned up in genome-wide screens for essential genes (3). Evidence from previous studies suggests that loss of *gumB* locks *S. marcescens* in a "stressed-out" state, leading to phenotypes consistent with an activated stress response, including loss of flagellum production, reduced secretion of toxins, and excess capsular polysaccharide synthesis (9, 11). These phenotypes are reminiscent of those of bacteria in a chronic infection or in biofilms and are associated with a less acute infection (12, 13). Consistent with this, mice infected with *S. enterica* that coded for partial-function IgaA protein were severely defective in systemic mouse infection models (14).

The constitutive activation of the Rcs systems in mutants defective in IgaA family proteins may confer increased bacterial persistence and resistance to the immune system. For example, in an *in vitro* experiment in which *E. coli* was serially passaged with phagocytic cells, the surviving *E. coli* cells were enriched for mutations in the *igaA* gene, which increased capsule production and resistance to phagocytosis (15). Mutations in *igaA* also have been characterized among multidrug-resistant clinical keratitis isolates of *E. coli* (16), together suggesting that mutation of *igaA* can aid in pathoadaptation and is clinically relevant. Consistent with this, the *igaA* gene was originally found in a screen for mutations that enabled *S. enterica* serovar Typhimurium to proliferate within fibroblast cells (17).

Because of the importance of IgaA-family protein GumB in *S. marcescens* proliferation in an invertebrate infection model, regulation of virulence factors, and cytotoxicity to corneal cells *in vitro* (9, 11), we tested the prediction that GumB and the Rcs system are crucial for corneal infections. In this study, we evaluated the importance of the Rcs system in *S. marcescens* keratitis using a rabbit keratitis model. Key findings were

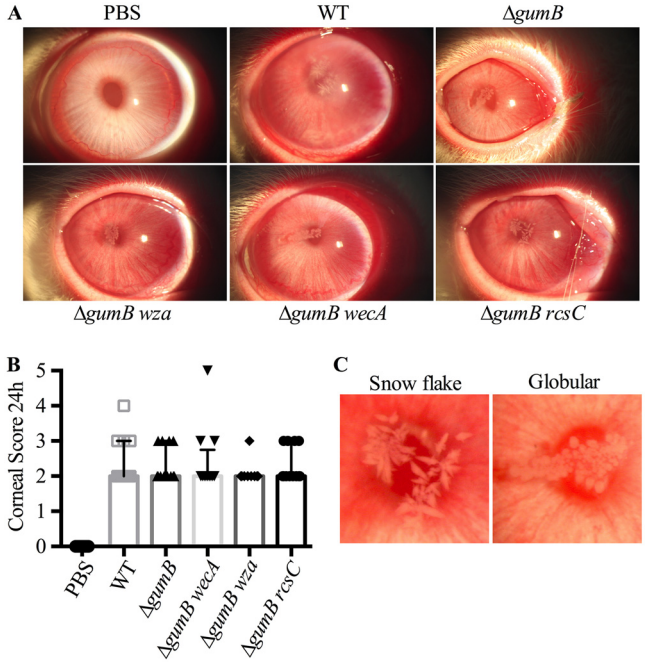

FIG 2 Rcs status of bacteria influences infiltrate morphology during *S. marcescens* corneal infections. (A) Representative images of infected eyes at 24 h postinfection. (B) Median values and interquartile ranges for clinical signs of inflammation 24 h after infection. (C) Representative images of typical infiltrate types.

retested using a human ocular surface cell line *in vitro*. Together, this study indicates that overactivation of a bacterial stress response system and the associated shift to phenotypes that mimic a chronic rather than acute infection lifestyle remarkably reduced that ability of the bacteria to cause corneal inflammation.

RESULTS

GumB is necessary for *S. marcescens* proliferation and inflammation in a rabbit corneal infection model. *S. marcescens* is a leading cause of contact lens-associated corneal infections (18, 19). Previous results using a keratitis isolate of *S. marcescens* indicated that constitutive activation of the Rcs stress response system, through mutation of the *gumB* gene, dramatically reduces the bacterium's ability to cause cytotoxicity *in vitro* using primary human corneal cells and virulence in an invertebrate pathogenesis model (11). However, the influence of the Rcs system on bacterial pathogenesis in a keratitis model is unknown. Cultures of *S. marcescens* WT contact lens-associated keratitis isolate K904 and an isogenic Δ*gumB* mutant were grown overnight in LB medium and diluted in phosphate-buffered saline (PBS), and ~500 CFU in 25 μl was injected into the corneal stroma. The actual injection was 468 ± 297 CFU for WT and 885 ± 550 CFU for the Δ*gumB* mutant.

At 24 and 48 h postinoculation, corneal and conjunctival clinical signs were examined by slit-lamp and evaluated using parameters from a modified MacDonald-Shadduck scoring system (20). At 24 h postinoculation, there was little difference in clinical inflammation scores for the cornea (Fig. 2A and B); however, the infiltrates were distinct. Corneas infected with the WT demonstrated a snowflake-like infiltrate in 11 out of 12 eyes, whereas the Δ*gumB* mutant-infected corneas had globular infiltrate in 11 out of 11 corneas (Fig. 2A and C).

At 48 h, corneal inflammation was higher for eyes infected with the WT than the Δ*gumB* mutant (Fig. 3). The corresponding corneal inflammatory scores were significantly higher ($P < 0.0001$, Kruskal-Wallis with Dunn's posttest) for the WT (median, 8.0; 95% confidence interval [CI], 7.13 to 8.21) than the Δ*gumB* mutant (median, 3.0; 95% CI, 2.44 to 4.36) (Fig. 3A). Corneal scores were the culmination of 0 to 4 for corneal opacity, area of corneal opacity, corneal vascularization, and corneal staining with fluorescein. Injection of PBS alone

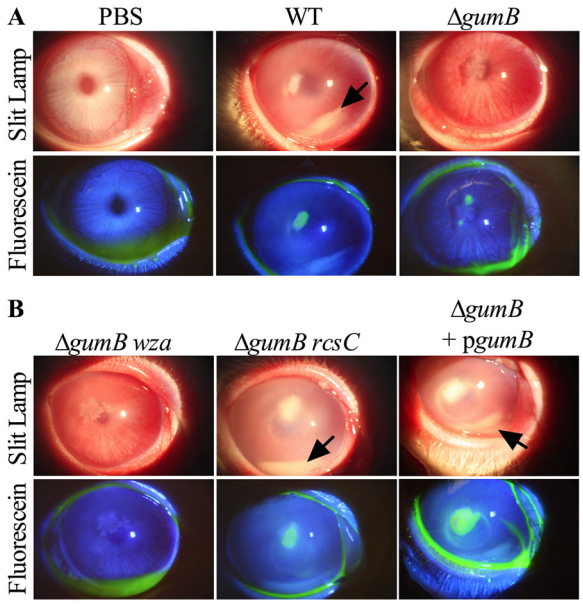

FIG 3 GumB is required for wild-type inflammation during *S. marcescens* corneal infections. Representative images of infected eyes at 48 h postinfection are shown. Fluorescein staining represents epithelial damage. The arrows indicate hypopyons.

as a negative control resulted in a score of 0 ± 0 (Fig. 3 and 4A). Rabbit eyes infected with WT *S. marcescens* presented with medium to large central corneal ulcers with fluorescein staining, indicating a loss of the epithelium (Fig. 3 and 4B). The Δ*gumB* mutant-infected eyes either had small ulcers or no ulcer. However, the epithelial defect area did not reach significance between the WT and Δ*gumB* mutant. The intact *gumB* gene on a medium-copy-number plasmid (370 ± 36 CFU injected per cornea, $n = 7$) was able to restore WT levels of corneal inflammation (median, 7.0; 95% CI, 5.70 to 7.16) and epithelial defect area, and, despite the lack of selection during the infection, 81% of recovered bacteria retained that plasmid after 48 h in the rabbit (Fig. 3 and 4A to D).

Other inflammatory signs included a loss of corneal clarity and the presence of hypopyons, a build-up of inflammatory cells in the anterior chamber (Fig. 3). Hypopyons are indicative of a high level of ocular inflammation and predictive of worse clinical outcomes (21, 22). Notably, 9 out of 12 eyes infected with the WT demonstrated a hypopyon (Fig. 3, arrow), compared to 0 out of 17 for PBS-injected eyes ($P = 0.0002$, Fisher's exact test) and 1 out of 11 for Δ*gumB* mutant-infected eyes ($P = 0.0028$ compared to the WT) (Fig. 4C and Table 1). In stark contrast, eyes infected with the Δ*gumB* mutant were generally clear, except for globular infiltrates (Fig. 3 and 4A). The *gumB* plasmid was able to complement this defect, with 7 out of 7 eyes having a hypopyon (Fig. 3 and 4C).

Conjunctival inflammatory scores followed a pattern similar to that of corneal scores, with WT-infected eyes having higher scores than the Δ*gumB* bacteria ($P < 0.01$, Kruskal-Wallis with Dunn's posttest) (Fig. 4D). The magnitude of the difference between WT- and Δ*gumB*-infected eyes was less extensive than that for corneal inflammation.

We assessed proinflammatory cytokines interleukin-1β (IL-1β) and tumor necrosis factor alpha (TNF-α) at the RNA level by NanoString technology in infected corneas at 24 h postinoculation (Fig. 5A). These cytokines are induced in tears and corneas from human patients with bacterial keratitis (23). Relative to the PBS-injected eyes and normalized by glyceraldehyde-3-phosphate dehydrogenase (GAPDH) levels, TNF-α transcripts were up 4.9-fold in WT-infected eyes compared to PBS-injected eyes and 5.7-fold compared to Δ*gumB* mutant-infected eyes ($P < 0.05$ by Mann-Whitney test). The effect was more dramatic for IL-1β, with a 363.8-fold increase in WT-infected eyes compared to PBS-injected eyes and 26.2-fold higher in the WT-infected eyes than Δ*gumB* mutant-infected eyes ($P < 0.05$, Mann-Whitney test) (Fig. 5A). Because the effect was greater for IL-1β, we evaluated IL-1β protein levels 48

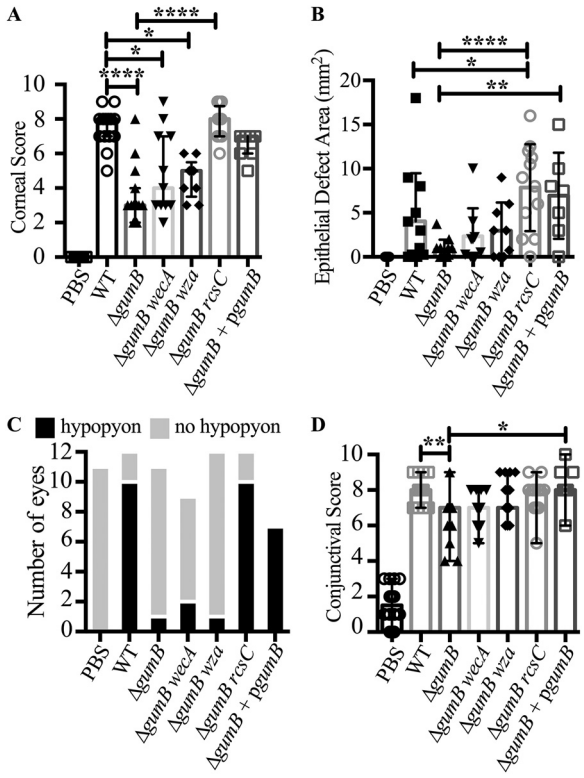

FIG 4 GumB and the Rcs system dictate the ability of *S. marcescens* to induce inflammation during corneal infection. Median values and interquartile ranges for clinical signs of inflammation 48 h after infection for cornea (A) and conjunctiva (D). The asterisks indicate significances by Kruskal-Wallis with Dunn's posttest. **, $P < 0.01$; ***, $P < 0.001$; ****, $P < 0.0001$. (B) Average and standard deviations from epithelial defects. ****, $P < 0.0001$, ANOVA with Tukey's posttest. (C) Enumeration of eyes with hypopyon.

h postinoculation by enzyme-linked immunosorbent assay (ELISA). A >1,000-fold increase in IL-1β was measured in WT-infected eyes compared to PBS-injected eyes ($P < 0.001$, analysis of variance [ANOVA] with Tukey's posttest) (Fig. 5B). Eyes infected with the Δ*gumB* mutant had a 56-fold elevation in IL-1β compared to PBS, but this did not reach significance. The Δ*gumB* mutant corneas had 19-fold reduced IL-1β compared to WT-infected corneas ($P < 0.01$) (Fig. 5B). The *gumB* plasmid complemented the Δ*gumB* mutant defect with increased induction of IL-1β compared to the Δ*gumB* mutant ($P < 0.001$) (Fig. 5B).

The bacterial burden, at 48 h postinfection, was 61-fold higher in the WT-infected corneas compared to those infected by the Δ*gumB* mutant (Fig. 5C) ($P < 0.01$, ANOVA with Tukey's posttest), and the *gumB* plasmid brought the CFU number to over 10^7 per cornea. These data demonstrate that *S. marcescens* can replicate from less than 10^3 to more than 10^7 in 48 h. This is notable because of the approximately 20 published studies testing mutant bacteria in the rabbit intrastromal injection model; only one other has demonstrated that a mutant bacterial strain had reduced proliferation compared to the isogenic WT (24, 25). Consistent with higher bacterial numbers and inflammatory scores, hematoxylin and

TABLE 1 Hypopyons were less prevalent in Δ*gumB* mutant-infected eyes

Strain	With hypopyon[a]	Without hypopyon[a]	*P* value vs WT[b]	*P* value vs PBS[b]
PBS	0	11	0.0001	NA
WT	10	2	NA	0.0001
Δ*gumB*	1	10	0.0006	1.0000
Δ*gumB wecA*	2	7	0.0092	0.1895
Δ*gumB wza*	1	11	0.0006	1.0000
Δ*gumB rcsC*	10	2	1.0000	0.0001

[a]Number of eyes with or without hypopyons or extensive fibrin in the anterior chamber.
[b]Two-tailed Fisher's exact test. NA, not applicable. Significant differences in boldface.

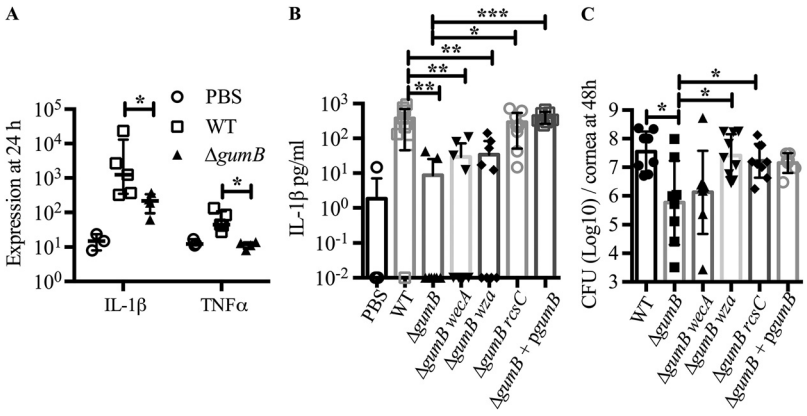

FIG 5 GumB mediates inflammation and proliferation within the rabbit cornea. (A) Median values and interquartile ranges are shown of RNA transcripts normalized by GAPDH RNA levels from corneas 24 h after infection. The asterisk indicates a *P* value of <0.05 for the WT versus Δ*gumB* mutant by Mann-Whitney test ($n = 3$ to 5 per group). (B) Mean and SD IL-1B protein levels measured by ELISA 48 h postinfection ($n = 8$ to 9 per group). **, $P < 0.01$ compared to the WT using ANOVA with Tukey's posttest. (C) Mean and standard deviation CFU per cornea at 48 h postinfection. Asterisks indicate a *P* value of <0.05 by ANOVA with Tukey's test.

eosin (H&E) staining of corneal sections showed epithelial defects, edema, and neutrophils in the WT-infected corneas (Fig. 6). By comparison, Δ*gumB* mutant-infected corneas had intact epithelial layers and relatively mild edema.

Role of capsule in GumB-mediated corneal infections. Mutation of IgaA-family proteins like *gumB* cause a major increase in production of extracellular polysaccharide (9). Here, we used previously described isogenic variants of the *gumB* mutant that do not make capsule due to mutations in capsule biosynthetic genes *wecA* and *wza* (9) to test for the importance of overproduction of capsule in the reduced corneal inflammation phenotype of the Δ*gumB* mutant. At 24 h, the *gumB wecA* double mutant produced inflammation indistinguishable from that of the other groups (Fig. 2), but at 48 h, Δ*gumB wza* and Δ*gumB wecA* mutants induced intermediate clinical corneal scores that were elevated compared to those of the Δ*gumB* mutant but were not significantly different from those of the Δ*gumB* mutant-injected eyes ($P > 0.05$ by Kruskal-Wallis with Dunn's posttest) (Fig. 3 and 4A). Epithelial defects and the frequency of hypopyons were similar to those of the Δ*gumB* mutant (Fig. 4B and C). IL-1β levels for the *gumB wecA* mutant were intermediate compared to those of the Δ*gumB* mutant and WT (Fig. 5B). CFU numbers were significantly elevated in the Δ*gumB wza* double mutant compared to the Δ*gumB* mutant (Fig. 5C). H&E staining of Δ*gumB wza* double mutant eyes was similar to that for Δ*gumB*-infected eyes but showed increased levels of neutrophils and a less robust epithelial layer (Fig. 6). Together, these suggest that overproduction of the capsule plays a relatively minor role in the Δ*gumB* mutant keratitis defects.

The Δ*gumB* mutant keratitis phenotype is reversed through inactivation of the Rcs pathway. Data indicate that the Δ*gumB* mutant has an overactive Rcs system and that mutation of *rcsB* or *rcsC* genes restores WT-like phenotypes to the Δ*gumB* mutant, such as ShlA-dependent cytotoxicity to corneal cells (11). This suggests that overactivation of the Rcs system is responsible for the reduced virulence of the Δ*gumB* mutant. To test whether the Rcs system is necessary for the Δ*gumB* mutant keratitis phenotype, we used a double mutant with a null mutation in the *rcsC* gene, a necessary component of Rcs signaling (Fig. 1). We isolated a Δ*gumB* mutant with a spontaneous duplication of 49 bp in the *rcsC* gene that creates an out-of-frame mutation. This allele was named *rcsC-SPV1*, for spontaneous pigmented variant number 1, and genetic experiments support that it codes for a loss of function mutation. For example, multicopy expression of the WT *rcsC* plasmid inhibits red pigment (prodigiosin) production. The WT was reduced in pigment production from 0.79 ± 0.17 (A_{534}/optical density at 600 nm [OD_{600}]) with the vector control to 0.05 ± 0.06 when expressing *rcsC* from a

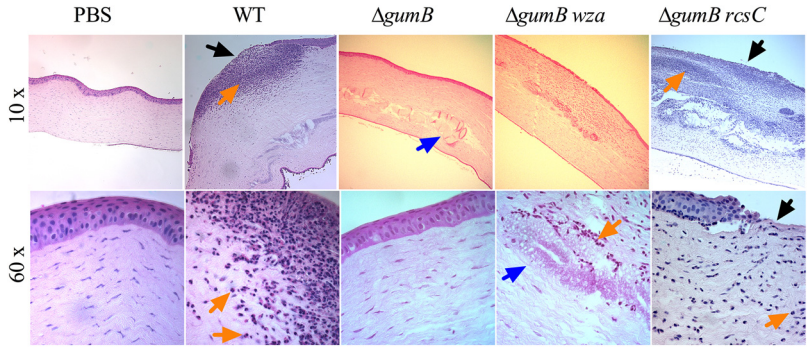

FIG 6 Histological analysis of *S. marcescens* infected corneas at 48 h. Representative images of hematoxylin- and eosin-stained corneal sections of eyes at 48 h postinfection. Large neutrophil infiltrates were observed in the WT- and Δ*gumB rcsC* mutant-infected eyes. The objective magnification is indicated. Black arrows indicate epithelial defects, blue arrows indicate globular infiltrates in Δ*gumB* mutant-infected corneas, and orange arrows indicate neutrophils.

multicopy plasmid. However, when the *rcsC-SPV1* allele gene with the 49-bp duplication was cloned and used in the same experiment, pigment levels were largely uninhibited (0.55 ± 0.15 [$n = 6$]). Genomic analysis also indicated that the Δ*gumB rcsC*-SPV1 strain had no mutations in other genes.

This Δ*gumB rcsC* double mutant was introduced into rabbit corneas (503 ± 448 CFU average inoculum) to test whether overactivation of the Rcs system due to *gumB* mutation was responsible for the Δ*gumB* mutant virulence defect. At 24 h postinoculation, the corneas infected with the Δ*gumB rcsC* double mutant had infiltrates similar to that of the WT, with 12 out of 12 infiltrates having a snowflake-like morphology (Fig. 2A and C). At 48 h, the corneal scores were indistinguishable between the Δ*gumB rcsC* and WT strains (Fig. 2 and 3A), and this was reflected in restored IL-1β levels that were significantly higher than those of Δ*gumB* mutant-infected eyes ($P < 0.05$, ANOVA with Tukey's posttest) (Fig. 5B), the presence of hypopyons (Fig. 4C), and the loss of corneal epithelium and numerous infiltrating neutrophils (Fig. 6). CFU numbers were similarly restored to the Δ*gumB* mutant by inactivation of the Rcs system ($P < 0.05$, ANOVA with Tukey's posttest) (Fig. 4C).

Two-component regulators can experience cross talk by which the phosphorylation state of the response regulator is altered by a noncognate histidine kinase (26), and data suggest that this can occur with the Rcs system, as Rcs-dependent transcription occurs at low levels in the absence of RcsC and RcsD (3). Therefore, we performed a second set of experiments using a pair of recently described isogenic *rcsB* deletion mutant strains, in which the entire *rcsB* open reading frame in the WT and Δ*gumB* mutant was replaced with the gene for a fluorescent protein, *mclover* (27). Additionally, as *rcsB* mutations are reported to have increased expression of the *shlBA* cytolysin operon, we generated a Δ*rcsB* Δ*shlB* double mutant to test whether Δ*rcsB* mutant phenotypes were dependent upon the ShlA/B toxin system. The ShlB protein is a transporter necessary for ShlA secretions, such that this Δ*shlB* mutant is phenotypically defective in ShlA-dependent phenotypes (11).

Approximately 1,000 CFU were injected per cornea, for a total of up to nine rabbits per group, over three separate experiments. Inocula were measured, and the WT had the highest number of CFU per eye, with an average of 1,015 ± 127 CFU, and the Δ*rcsB* mutant had the lowest, with 845 ± 176. There were no significant differences between injected CFU numbers for any group, as measured by ANOVA with Tukey's posttest ($P < 0.05$).

Conjunctival inflammation was observed for all groups except the PBS control, including redness, chemosis, and discharge (Fig. 7). There were no significant differences between genotypes with respect to conjunctival inflammation at 24 or 48 h, except for eyes infected with the Δ*rcsB* Δ*shlB* double mutant compared to the Δ*rcsB* mutant at 48 h ($P < 0.05$, Kruskal Wallis with Dunn's posttest) (Fig. 7 and 8A and not shown). For the cornea, the Δ*gumB* Δ*rcsB* and Δ*rcsB* mutants had a higher level of

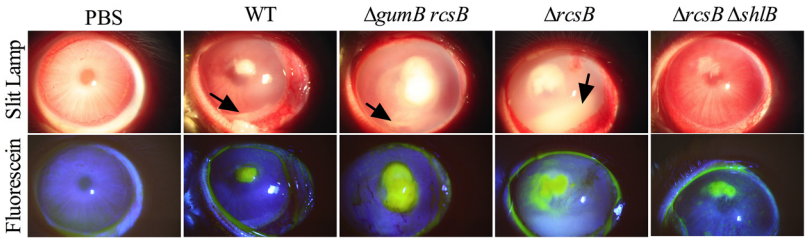

FIG 7 Corneas infected with *S. marcescens* defective in the Rcs system have severe keratitis, and mutation of the *shlB* cytolysin transporter reverses the Δ*rcsB* mutant hypervirulent phenotype. Representative images of infected eyes at 48 h postinfection are shown. Fluorescein staining represents epithelial damage. The arrows indicate hypopyons.

inflammation at 24 h postinjection than the Δ*rcsB* Δ*shlB* double mutant, which was indistinguishable from PBS-injected corneas (Fig. 8B). The snowflake infiltrate was observed in 7/7 for WT-infected eyes, 2/8 for Δ*gumB* Δ*rcsB* mutant, 9/9 for Δ*rcsB* mutant, and 9/9 for Δ*rcsB* Δ*shlB* mutant; the Δ*gumB* Δ*rcsB* mutant was significantly different from the other groups by Fisher's exact test ($P \leq 0.007$). By 48 h, the Δ*rcsB* Δ*shlB* strain had lower inflammatory scores than the other strains, and these were significantly lower than those of the Δ*rcsB* group ($P < 0.01$) (Fig. 8C).

As was shown in the experiment described above, the majority of WT *S. marcescens* strain K904-infected eyes had hypopyons at 48 h (Fig. 8D), as did Δ*gumB* Δ*rcsB* and Δ*rcsB* mutants. There were no significant differences in epithelial defect size ($P > 0.05$); however, the Δ*gumB* Δ*rcsB*- and Δ*rcsB*-infected eyes had the largest average erosion areas at 11.7 and 10.6 mm^2, the WT was intermediate at 9.6 mm^2, and the Δ*rcsB* Δ*shlB* mutant induced the smallest defects at 6.7 mm^2. In contrast, the Δ*rcsB* Δ*shlB* double mutants were remarkably reduced in causing inflammation sufficient to produce hypopyons (Fig. 8D) ($P < 0.0152$ compared to WT and $P < 0.0023$ compared to Δ*rcsB* mutant by Fisher's exact test). All groups except the Δ*rcsB* Δ*shlB* mutant had significantly more ability to induce hypopyons than PBS-injected eyes ($P < 0.023$ by Fisher's exact test). With respect to the proinflammatory cytokine IL-1B, the Δ*rcsB* mutant induced more IL-1β production than the WT ($P < 0.05$, Tukey's posttest), and the level for the Δ*rcsB* Δ*shlB* mutant was significantly lower than that for the Δ*rcsB* mutant ($P < 0.0001$) (Fig. 8E). The CFU numbers per cornea at 48 h postinjection were largely similar, with the exception of the Δ*gumB* Δ*rcsB* double mutant having significantly lower counts per cornea ($P < 0.05$) than the other groups.

Cytotoxicity to human corneal cells and IL-1β induction are Rcs system controlled. A human corneal epithelial cell line (HCLE) was used to test whether the effect of various mutations on *S. marcescens* virulence in the rabbit keratitis model were reproduced with human cells *in vitro*. Cells were challenged with WT and mutant bacteria at a multiplicity of infection (MOI) of 2, 20, 50, and 200 and coincubated for 2 h, and cytotoxicity was measured using a resazurin-based assay as previously described and validated with orthogonal methods (9, 11) (Fig. 9A). The WT killed nearly all HCLE cells at an MOI of 20 or greater but was reduced to approximately 25% killing at an MOI of 2. The Δ*gumB* mutant was defective in cytotoxicity even at an MOI of 200. The Δ*rcsB* and Δ*gumB* Δ*rcsB* strains were approximately twice a cytotoxic as the WT at an MOI of 2 ($P < 0.05$). Elimination of ShlA secretion by the Δ*rcsB* mutant reduced its cytotoxicity completely (Δ*rcsB* Δ*shlB* mutant). Similarly, a Δ*shlB* mutant was not cytotoxic. IL-1β levels were elevated in corneal cells challenged with WT bacteria but not the Δ*gumB* mutant (Fig. 9B). Together, these findings mirror the trends observed in the rabbit keratitis model.

DISCUSSION

Microbial keratitis, though generally treatable with antibiotics, still leads to vision loss. This is due to the rapid growth of the organism before treatment and continued damage to corneal tissue by inflammatory cells even after the death of the microbes (28–32). In human

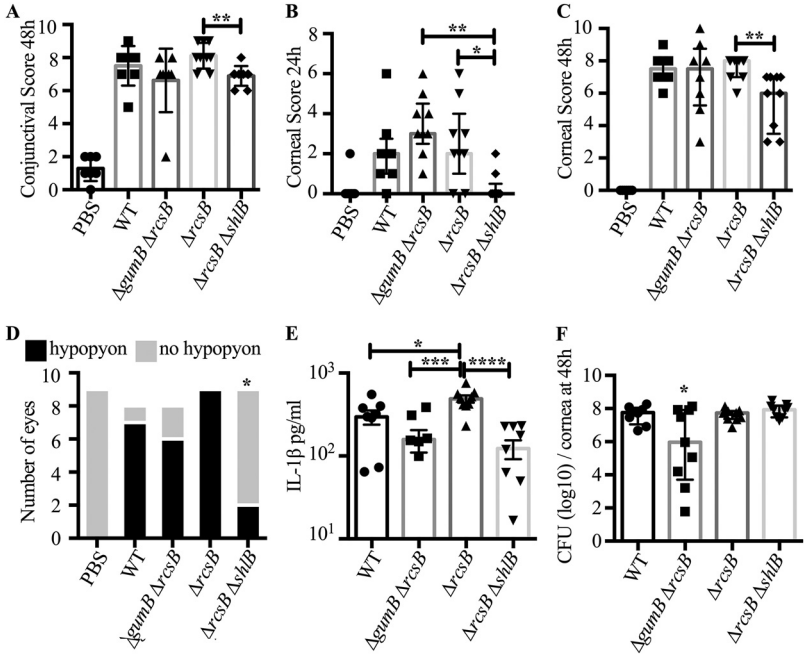

FIG 8 Rcs system influences the ability of *S. marcescens* to induce inflammation during corneal infection. (A to C) Median values and interquartile ranges for clinical signs of inflammation at 24 or 48 h after infection for conjunctiva (A) and cornea (B and C). The asterisks indicate significance by Kruskal-Wallis test with Dunn's posttest. (D) Enumeration of eyes with and without hypopyons. The asterisk indicates significantly fewer eyes with hypopyons than all other groups, except PBS, by Fisher's exact test. (E and F) Mean and standard deviation IL-1β cytokines per cornea and CFU per cornea; asterisks indicate differences by ANOVA with Tukey's posttest. For panel F, the asterisk indicates significantly fewer CFU per cornea than the other groups. $n = 7$ to 9 per group from a total of three independent experiments. *, $P < 0.05$; **, $P < 0.01$; ***, $P < 0.001$; ****, $P < 0.0001$.

patients, *S. marcescens* is a leading cause of contact lens-associated keratitis and can lead to vision loss and, in rare cases, blindness (18, 19). *S. marcescens* has been shown to readily infect the corneas of rabbits (33–35). It is highly inflammatory, and its lipopolysaccharide and purified proteases are sufficient to induce keratitis (34, 36–39). In a mouse keratitis model, it was demonstrated that the cornea requires TLR4, TLR5, IL-1R, and MyD88 to effectively clear *S. marcescens* infections (40), suggesting that flagellin and lipopolysaccharide are important pathogen-associated molecular patterns (PAMPs) of *S. marcescens* in the cornea. Nevertheless,

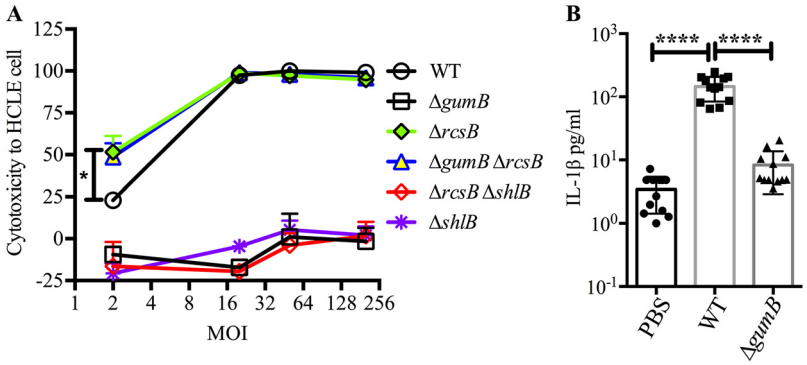

FIG 9 Human corneal cell susceptibility and cytokine response to *S. marcescens*. (A) Cell viability was evaluated following 2-h challenge by *S. marcescens* and mutants at MOIs of 2, 20, 50, and 200. At an MOI of 2, the Δ*rcsB* and Δ*gumB* Δ*rcsB* mutants were more cytotoxic than the WT. At all MOIs, the Δ*gumB*, Δ*shlB*, and Δ*rcsB* Δ*shlB* mutants were less cytotoxic than the WT. *n*, 3. (B) IL-1β analysis of HCLE cells exposed to normalized bacterial supernatants for 5 h and measured using BioLegend flow-based ELISA. *n*, 12. Means and SD are shown. Asterisks indicate significant differences by ANOVA with Tukey's posttest. *, $P < 0.05$; **, $P < 0.01$; ****, $P < 0.0001$.

the only *S. marcescens* gene directly tested for a role in keratitis using mutant bacterial strains has been the transcription factor *eepR* (41).

The purpose of this study was to establish whether the IgaA-family protein GumB from *S. marcescens* and the related Rcs stress response system play a role in microbial pathogenesis during bacterial keratitis. Data from this study demonstrated that a clinical keratitis isolate of *S. marcescens* with a constitutively active Rcs system (Δ*gumB* mutant) diminished the ability of the bacterium to proliferate in the cornea, with a 1.875-$\log_{10}$ (98%) loss of CFU in *gumB*-infected corneas relative to those infected by the WT. A reduction in CFU numbers for a mutant strain of any bacterial species compared to an isogenic strain in the rabbit corneal intrastromal model is rare in the literature, with only one previous example from the approximately 20 previous studies using mutant bacteria in rabbit intrastromal infection models. The other was the *eepR* mutant of *S. marcescens* (41). More clinically significant was that the Δ*gumB* mutant was defective in causing corneal inflammation, judged by corneal inflammatory signs, with a 62.5% reduction in corneal inflammatory scores. These correlated with reduced production of proinflammatory cytokines IL-1β and TNF-α and neutrophil infiltration into the cornea. Moreover, the near absence of hypopyons in the Δ*gumB* mutant-infected eyes is clinically relevant, as hypopyons are risk factors for poor vision outcome and for surgical intervention in human patients with bacterial keratitis (22, 42, 43).

Complementation of the *gumB* mutation with WT *gumB* gene on a plasmid reversed the Δ*gumB* mutant defects. This indicated that the reduced virulence phenotypes of the mutant strain were due to loss of GumB function rather than other mutations or polar effect of the deletion mutation.

The WT and strains with an inactivated Rcs system (*rcsB* and *rcsC* mutants) induced infiltrates with a snowflake appearance at 24 h that were reminiscent of the presentation of infectious crystalline keratopathy, in which microbes are thought to form biofilms that spread along the lamelar planes of the corneal stroma that create a crystalline or snowflake-like pattern (44). This suggests that WT and Rcs-defective strains penetrate into the cornea along the lamellar planes, whereas the Rcs-overexpressing Δ*gumB* mutant does not. The difference in spreading may be due to lack of swimming and swarming motility previously demonstrated for the Δ*gumB* mutant in *S. marcescens* and other mutation of genes for IgaA orthologs in members of the *Enterobacterales* (9, 45, 46).

The Δ*gumB* mutant, like *igaA* mutants of *Salmonella*, generated highly mucoid colonies due to overproduction of capsular polysaccharide (9). Our results suggest that overexpression of the *S. marcescens* capsular polysaccharide contributes to the reduced inflammation caused by the Δ*gumB* mutant, as revealed by intermediate corneal inflammatory phenotypes in the Δ*gumB* mutant in which the capsular polysaccharide genes *wecA* and *wza* were mutated (both being required for the extracellular capsule); although the measurements did not reach significance, there was an upward trend in all experiments with the capsule mutants compared to the Δ*gumB* mutant. In the Δ*gumB* mutant background, capsule overproduction may prevent the immune system from recognizing bacterial surface PAMPs, leading to the reduced inflammation observed with the Δ*gumB* mutant-infected eyes. However, the lower CFU number from the Δ*gumB* mutant suggests that the excess capsule did not promote survival versus phagocytic cells. A previous study demonstrated that the macrophage-like RAW cell line was less efficient at phagocytosing the Δ*gumB* mutant than the WT, and that the WT, but not the Δ*gumB* mutant, could proliferate within the phagocytic cells (11). These data suggest that for the *S. marcescens* Δ*gumB* mutant, excess capsule can reduce the frequency of being taken up but is not sufficient for intracellular growth. Nevertheless, the ability of the Δ*gumB wza* and *wecA* double mutants to mount a successful infection in the rabbit corneas indicates that the capsule is not a strict requirement for *S. marcescens* to infect the eye. The necessity of bacterial capsules during corneal infection has only been studied using isogenic strains with the Gram-positive bacterium *Streptococcus pneumoniae*. Marquart and colleagues demonstrated that *S. pneumoniae* has to be alive to cause ocular inflammation and that a capsule mutant

was equally virulent to the capsulated WT in a rabbit keratitis model (47, 48). Furthermore, it is feasible that mutations in capsule biosynthetic genes could activate the Rcs system, as was shown in a WT *S. marcescens* strain (49). Since, under specific circumstances, the Rcs system can be activated in an IgaA (GumB)-independent manner (3), it is possible that the *wecA* and *wza* mutation activation of the Rcs system activates the Rcs system beyond what is observed for the Δ*gumB* mutation. However, this is expected to have a relatively minor impact, as the Rcs-dependent phenotypes of the Δ*gumB* mutant are already pronounced.

Whereas activation of the Rcs system through mutation of *gumB* led to reduced virulence, the inactivation of the Rcs system in the Δ*gumB* Δ*rcsB*, Δ*gumB rcsC*, and Δ*rcsB* mutants restored virulence to equal to or higher than that of the WT. Similarly, in a bacteremia model, *rcsB* mutants caused higher mortality to mice in a capsule-independent manner (6). Anderson and colleagues suggested that elevated *shlBA* expression in the *rcsB* mutant is responsible for the increased virulence (6). This conclusion was partially based on previous evidence describing that *rssAB* mutants, which have higher *shlBA* expression, caused higher mortality rates and more severe pathogenesis in a rat lung infection model (50), and that RcsB is a negative regulator of *shlBA* (51). Together, these observations suggested that in *S. marcescens*, the intact Rcs system act to modulate virulence, perhaps resulting in reduced immune activation and mortality of the host. Interestingly, species of the *Enterobacterales* reported to have higher virulence in Rcs-defective strains have ShlA orthologs (*E. tarda*, *P. mirabilis*, and *S. marcescens*), whereas those species reported to have reduced virulence conferred by *rcs* mutations typically do not have ShlA orthologs (*E. coli*, *C. rodentium*, and *S. enterica*). Future studies will evaluate the direct role of the ShlA toxin in ocular infections. However, it was clear that the strong Δ*rcsB* virulent phenotype required ShlA, as the Δ*rcsB* Δ*shlB* double mutant had significantly reduced corneal inflammation. It is also noticeable that the Δ*rcsB* Δ*shlB* defective strain attained a higher burden in the cornea than the WT. Similar trends have been reported for bacteria defective in production of other pore-forming toxins in the rabbit keratitis model, including an alpha-toxin mutant of *S. aureus* (52) and a pneumolysin mutant of *S. pneumoniae* (53).

In a previous study, the Δ*gumB* mutant was nearly completely avirulent in an invertebrate infection model, with an approximately 4-$\log_{10}$ reduction in CFU numbers compared to the WT (11), whereas in the rabbit cornea they are reduced in proliferation by almost 2 $\log_{10}$ CFU. In both cases the Δ*gumB* mutant was reduced in microbial pathogenesis, suggesting that the *G. mellonella* model was predictive of the mammalian model. The Δ*gumB* mutant has similar growth characteristics in minimal and rich media (9) and *G. mellonella* homogenates (11), suggesting that the observed defect was not due to reduced ability to utilize nutrients. However, altered production of enzymes or toxins involved in nutrient acquisition, such as ShlA, in the *in vivo* environment could account for the lowered CFU numbers.

The *in vitro* studies here support previous observations that the Δ*gumB* mutant is defective in cytotoxicity to HCLE cells even at high MOI (11), but they go further in demonstrating the elevated cytotoxic potential of the Δ*rcsB* mutant and the Δ*gumB* Δ*rcsB* mutant, which agrees with the *in vivo* studies presented here. Furthermore, they show that the Δ*rcsB* cytotoxic phenotype is ShlA secretion dependent, as the Δ*rcsB* Δ*shlB* double mutant was completely attenuated for cytotoxicity. Consistent with the rabbit keratitis model, the Δ*gumB* mutant was defective in IL-1β induction from human ocular surface cells *in vitro*.

The *in vivo* factors that activate the Rcs system are not fully understood but include lysozyme and cationic peptides (3). Both of these are key features of the innate defenses of the ocular surface (54). It is likely that after infection is established, it would benefit *S. marcescens* to activate the Rcs system, which would reduce PAMP and toxin production and increase capsule production. A temporal role for controlled regulation of the Rcs system in biofilm formation and pathogenicity was suggested by Huang et al. (55). However, during early stages, it is probable that some Rcs-inhibited factors contribute to establishing infection such as flagellin and ShlA. Thus, a well-coordinated balance in activity of the Rcs

TABLE 2 Strains and plasmids used in this study

Strain or plasmid	Description	Source or reference
Strains		
K904	Contact lens-associated keratitis isolate (WT)	61
CMS4001	K904 Δ*gumB*	9
CMS4236	K904 Δ*shlB*	11
CMS4619	K904 Δ*gumB wecA*; capsule deficient	9
CMS4214	K904 Δ*gumB wza*; capsule deficient	9
CMS4141	K904 Δ*gumB rcsC-SPV1*; Rcs system defective	This study
CMS5163	K904 Δ*gumB* Δ*rcsB*::mclover	27
CMS5177	K904 Δ*rcsB*::mclover	27
CMS5356	K904 Δ*rcsB* Δ*shlB*	This study
Plasmids		
pMQ132	broad host range shuttle vector oripBBR1	62
pMQ460	allelic replacement vector with sacB and I-SceI	25
pMQ473	pMQ460 with Δ*shlB* allele	11
pMQ480	pMQ132 with *gumB* gene under control of P_{lac}	9
pMQ615	pMQ132 with *rcsC* gene under control of P_{lac}	11
pMQ616	pMQ132 with *rcsC-SPV1* allele under control of P_{lac}	This study

system is likely required for effective pathogenesis by *S. marcescens*. Consistent with this idea, the key Rcs system transcription factor, RcsB, not only is modulated in activity by its cognate histidine kinase but also has numerous binding partners that fine tune its activity, such as RcsA (3). In summary, this study solidifies the role for GumB and the Rcs system as having an important role in ocular bacterial host-pathogen interactions.

MATERIALS AND METHODS

Bacterial strains, culture conditions, and molecular biology. Bacterial strains are listed in Table 2 and were maintained at −80°C. Bacteria were streaked to single colonies, and individual colonies were used to inoculate LB medium (56). Gentamicin was used at 10 μg/ml to select for plasmid maintenance.

The Δ*gumB rcsC* isolate (strain CMS4141) was isolated as a genetic suppressor of Δ*gumB* pigment phenotype (to be described elsewhere). The *rcsC* mutant gene was cloned in vector pMQ132 using primers and methods previously described (11). The mutation in *rcsC*, noted as *rcsC-SPV1*, was determined using Sanger sequencing of the *rcsC* gene (University of Pittsburgh Genomics Research Core).

Two-step allelic replacement was used to delete the *shlB* gene in the Δ*rcsB* strain as previously described using pMQ473 and verified by PCR as previously described (11).

Genomic DNA from the K904 and CMS4141 (Δ*gumB rcsC*-SPV1) strains were isolated using a GenElute bacterial genomic DNA kit (Sigma) and sequenced by MiGsCenter, Inc. (Pittsburgh, PA), by Illumina NextSeq 500 (both genomes), Illumina MiSeq (K904 genome), and Oxford Nanopore (K904 genome), to be described elsewhere. Variant calling was performed by MiGsCenter, Inc., using breseq software v0.31.0 using default parameters (57), and no differences in open reading frames were found.

Microbial keratitis studies. The present study conformed to the ARVO Statement on the Use of Animals in Ophthalmic and Vision Research. The study was approved by the University of Pittsburgh Institutional Animal Care and Use Committee (IACUC protocol 16098925B). For infection experiments, bacteria were grown overnight at 30°C with aeration, normalized by optical density (600 nm), adjusted to ~500 CFU in 25 μl, and injected into the right corneas of New Zealand White rabbits. Actual inocula colony counts were determined using the EddyJet 2 spiral plating system (Neutec Group Inc., Farmingdale, NY) on Trypticase agar with 5% sheep's blood plates. The plates were incubated overnight at 30°C, and the colonies were using the automated Flash and Grow colony counting system (Neutec Group, Inc.). At 24 and 48 h postinjection, eyes were evaluated for ocular signs of inflammation using a slit-lamp according to a modified MacDonald-Shadduck grading system (20). After sacrifice, corneas were harvested with a 10-mm trephine and homogenized with an MP Fast Prep-24 homogenizer using lysing matrix A tubes (MP Biomedicals), and bacteria were enumerated by dilution plating as described above. Homogenates were clarified by centrifugation (10 min at 16,000 to 21000 × *g*) and stored at −20°C until used for ELISA analysis for proinflammatory markers by following the manufacturers' protocols (58, 59). For IL-1β analysis, Sigma-Aldrich product RAB1108 was used.

For histological analysis, corneas were fixed in 4% paraformaldehyde in phosphate-buffered saline (pH 7.4) and embedded in paraffin. Central corneal sections were generated (5 μm) and stained with hematoxylin and eosin staining. Slides were imaged using the Olympus Provis AX-70 microscope with MagnaFire 2.1 software.

Cell culture studies. Bacteria were grown overnight in LB medium, adjusted to an OD_{600} of 1.0 in keratinocyte serum-free medium (ThermoFisher), and adjusted to various MOIs as indicated and challenged for 2 h. Cytotoxicity to HCLE cells (60) was measured as previously described, using PrestoBlue cell viability reagent (ThermoFisher) as previously described (11).

IL-1β was measured from HCLE cells after 5 h of incubation with filter-sterilized bacterial supernatants from cultures normalized to an OD_{600} of 2 using a human LegendPlex kit (BioLegend) according to the manufacturer's specifications and using a CytoFLEX LX instrument (Beckman Coulter). Data were analyzed using LegendPlex data analysis software (BioLegend).

Statistical analysis. Data were analyzed using GraphPad Prism software. Nonparametric analysis was used to analyze inflammatory scores by Kruskal-Wallis analysis with Dunn's posttest, and ANOVA with Tukey's posttest or Student's *t* test was used to analyze other experimental data. Fisher's exact test was used to compare eyes with hypopyons. In all cases $P < 0.05$ was considered significant.

ACKNOWLEDGMENTS

We thank Kimberly Brothers, Jake Callaghan, and Katherine Davoli for expert technical help, Kira Lathrop, the Center for Biologic Imaging, Katherine Helfrich, and Mark Ross for microscopy help, and Vaughn Cooper and Dan Synder for sequencing and analysis expertise.

This study was supported by the Charles T. Campbell Laboratory of Ophthalmic Microbiology, NIH grants EY027331 (to R.M.Q.S.) and EY08098 (Core Grant for Vision Research), the Eye and Ear Foundation of Pittsburgh, and unrestricted funds from Research to Prevent Blindness.

REFERENCES

1. Griffiths M. 2005. Understanding pathogen behaviour: virulence, stress response, and resistance. CRC Press, Boca Raton, FL.
2. Flores-Kim J, Darwin AJ. 2014. Regulation of bacterial virulence gene expression by cell envelope stress responses. Virulence 5:835–851. https://doi.org/10.4161/21505594.2014.965580.
3. Wall E, Majdalani N, Gottesman S. 2018. The complex Rcs regulatory cascade. Annu Rev Microbiol 72:111–139. https://doi.org/10.1146/annurev-micro-090817-062640.
4. Howery KE, Clemmer KM, Rather PN. 2016. The Rcs regulon in *Proteus mirabilis*: implications for motility, biofilm formation, and virulence. Curr Genet 62:775–789. https://doi.org/10.1007/s00294-016-0579-1.
5. Xu Y, Xu T, Wang B, Dong X, Sheng A, Zhang XH. 2014. A mutation in *rcsB*, a gene encoding the core component of the Rcs cascade, enhances the virulence of *Edwardsiella tarda*. Res Microbiol 165:226–232. https://doi.org/10.1016/j.resmic.2014.02.006.
6. Anderson MT, Mitchell LA, Zhao L, Mobley HLT. 2017. Capsule production and glucose metabolism dictate fitness during *Serratia marcescens* bacteremia. mBio 8:e00740-17. https://doi.org/10.1128/mBio.00740-17.
7. Lasaro M, Liu Z, Bishar R, Kelly K, Chattopadhyay S, Paul S, Sokurenko E, Zhu J, Goulian M. 2014. *Escherichia coli* isolate for studying colonization of the mouse intestine and its application to two-component signaling knockouts. J Bacteriol 196:1723–1732. https://doi.org/10.1128/JB.01296-13.
8. Wang D, Korban SS, Pusey PL, Zhao Y. 2011. Characterization of the RcsC sensor kinase from Erwinia amylovora and other Enterobacteria. Phytopathology 101:710–717. https://doi.org/10.1094/PHYTO-09-10-0258.
9. Stella NA, Brothers KM, Callaghan JD, Passerini AM, Sigindere C, Hill PJ, Liu X, Wozniak DJ, Shanks RMQ. 2018. An IgaA/UmoB-family protein from *Serratia marcescens* regulates motility, capsular polysaccharide, and secondary metabolite production. Appl Environ Microbiol 84:e02575-17. https://doi.org/10.1128/AEM.02575-17.
10. Dufour A, Furness RB, Hughes C. 1998. Novel genes that upregulate the *Proteus mirabilis flhDC* master operon controlling flagellar biogenesis and swarming. Mol Microbiol 29:741–751. https://doi.org/10.1046/j.1365-2958.1998.00967.x.
11. Brothers KM, Callaghan JD, Stella NA, Bachinsky JM, AlHigaylan M, Lehner KL, Franks JM, Lathrop KL, Collins E, Schmitt DM, Horzempa J, Shanks RMQ. 2019. Blowing epithelial cell bubbles with GumB: shlA-family pore-forming toxins induce blebbing and rapid cellular death in corneal epithelial cells. PLoS Pathog 15:e1007825. https://doi.org/10.1371/journal.ppat.1007825.
12. Balasubramanian D, Schneper L, Kumari H, Mathee K. 2013. A dynamic and intricate regulatory network determines *Pseudomonas aeruginosa* virulence. Nucleic Acids Res 41:1–20. https://doi.org/10.1093/nar/gks1039.
13. Rahim K, Saleha S, Zhu X, Huo L, Basit A, Franco OL. 2017. Bacterial contribution in chronicity of wounds. Microb Ecol 73:710–721. https://doi.org/10.1007/s00248-016-0867-9.
14. Dominguez-Bernal G, Pucciarelli MG, Ramos-Morales F, Garcia-Quintanilla M, Cano DA, Casadesus J, Garcia-del Portillo F. 2004. Repression of the RcsC-YojN-RcsB phosphorelay by the IgaA protein is a requisite for *Salmonella* virulence. Mol Microbiol 53:1437–1449. https://doi.org/10.1111/j.1365-2958.2004.04213.x.
15. Miskinyte M, Sousa A, Ramiro RS, de Sousa JA, Kotlinowski J, Caramalho I, Magalhaes S, Soares MP, Gordo I. 2013. The genetic basis of *Escherichia coli* pathoadaptation to macrophages. PLoS Pathog 9:e1003802. https://doi.org/10.1371/journal.ppat.1003802.
16. Van Tyne D, Ciolino JB, Wang J, Durand ML, Gilmore MS. 2016. Novel phagocytosis-resistant extended-spectrum beta-lactamase-producing *Escherichia coli* from keratitis. JAMA Ophthalmol 134:1306–1309. https://doi.org/10.1001/jamaophthalmol.2016.3283.
17. Cano DA, Martinez-Moya M, Pucciarelli MG, Groisman EA, Casadesus J, Garcia-Del Portillo F. 2001. *Salmonella enterica* serovar Typhimurium response involved in attenuation of pathogen intracellular proliferation. Infect Immun 69:6463–6474. https://doi.org/10.1128/IAI.69.10.6463-6474.2001.
18. Mah-Sadorra JH, Najjar DM, Rapuano CJ, Laibson PR, Cohen EJ. 2005. *Serratia* corneal ulcers: a retrospective clinical study. Cornea 24:793–800. https://doi.org/10.1097/01.ico.0000159738.06167.88.
19. Das S, Sheorey H, Taylor HR, Vajpayee RB. 2007. Association between cultures of contact lens and corneal scraping in contact lens related microbial keratitis. Arch Ophthalmol 125:1182–1185. https://doi.org/10.1001/archopht.125.9.1182.
20. Altmann S, Emanuel A, Toomey M, McIntyre K, Covert J, Dubielzig RR, Leatherberry G, Murphy CJ, Kodihalli S, Brandt CR. 2010. A quantitative rabbit model of vaccinia keratitis. Invest Ophthalmol Vis Sci 51:4531–4540. https://doi.org/10.1167/iovs.09-5106.
21. Chidambaram JD, Venkatesh Prajna N, Srikanthi P, Lanjewar S, Shah M, Elakkiya S, Lalitha P, Burton MJ. 2018. Epidemiology, risk factors, and clinical outcomes in severe microbial keratitis in South India. Ophthalmic Epidemiol 25:297–305. https://doi.org/10.1080/09286586.2018.1454964.
22. Miedziak AI, Miller MR, Rapuano CJ, Laibson PR, Cohen EJ. 1999. Risk factors in microbial keratitis leading to penetrating keratoplasty. Ophthalmology 106:1166–1170. https://doi.org/10.1016/S0161-6420(99)90250-6.
23. Konstantopoulos A, Del Mar Cendra M, Tsatsos M, Elabiary M, Christodoulides M, Hossain P. 2020. Morphological and cytokine profiles as key parameters to distinguish between Gram-negative and Gram-positive bacterial keratitis. Sci Rep 10:20092. https://doi.org/10.1038/s41598-020-77088-w.
24. O'Callaghan RJ, Engel LS, Hobden JA, Callegan MC, Green LC, Hill JM. 1996. *Pseudomonas* keratitis. The role of an uncharacterized exoprotein, protease IV, in corneal virulence. Invest Ophthalmol Vis Sci 37:534–543.
25. Stella NA, Lahr RM, Brothers KM, Kalivoda EJ, Hunt KM, Kwak DH, Liu X, Shanks RM. 2015. *Serratia marcescens* cyclic AMP-receptor protein controls transcription of EepR, a novel regulator of antimicrobial secondary metabolites. J Bacteriol 197:2468–2478. https://doi.org/10.1128/JB.00136-15.
26. Agrawal R, Sahoo BK, Saini DK. 2016. Cross-talk and specificity in two-component signal transduction pathways. Future Microbiol 11:685–697. https://doi.org/10.2217/fmb-2016-0001.
27. Lehner KM, Stella NA, Calvario RC, Shanks RMQ. 2020. *mClover*Blaster: a tool to make markerless deletions and fusion using lambda red and I-SceI

in Gram-negative bacterial genomes. J Microbiol Methods 178:106058. https://doi.org/10.1016/j.mimet.2020.106058.
28. Hazlett LD. 2005. Role of innate and adaptive immunity in the pathogenesis of keratitis. Ocul Immunol Inflamm 13:133–138. https://doi.org/10.1080/09273940490912362.
29. Willcox MD. 2007. *Pseudomonas aeruginosa* infection and inflammation during contact lens wear: a review. Optom Vis Sci 84:273–278. https://doi.org/10.1097/OPX.0b013e3180439c3e.
30. Pearlman E, Sun Y, Roy S, Karmakar M, Hise AG, Szczotka-Flynn L, Ghannoum M, Chinnery HR, McMenamin PG, Rietsch A. 2013. Host defense at the ocular surface. Int Rev Immunol 32:4–18. https://doi.org/10.3109/08830185.2012.749400.
31. Lakhundi S, Siddiqui R, Khan NA. 2017. Pathogenesis of microbial keratitis. Microb Pathog 104:97–109. https://doi.org/10.1016/j.micpath.2016.12.013.
32. Lin A, Rhee MK, Akpek EK, Amescua G, Farid M, Garcia-Ferrer FJ, Varu DM, Musch DC, Dunn SP, Mah FS, American Academy of Ophthalmology Preferred Practice Pattern Cornea and External Disease Panel. 2019. Bacterial keratitis preferred practice pattern. Ophthalmology 126:P1–P55. https://doi.org/10.1016/j.ophtha.2018.10.018.
33. Lyerly D, Gray L, Kreger A. 1981. Characterization of rabbit corneal damage produced by *Serratia* keratitis and by a serratia protease. Infect Immun 33:927–932. https://doi.org/10.1128/IAI.33.3.927-932.1981.
34. Kamata R, Matsumoto K, Okamura R, Yamamoto T, Maeda H. 1985. The serratial 56K protease as a major pathogenic factor in serratial keratitis. Clinical and experimental study. Ophthalmology 92:1452–1459. https://doi.org/10.1016/s0161-6420(85)33855-1.
35. Hume EB, Conerly LL, Moreau JM, Cannon BM, Engel LS, Stroman DW, Hill JM, O'Callaghan RJ. 1999. *Serratia marcescens* keratitis: strain-specific corneal pathogenesis in rabbits. Curr Eye Res 19:525–532. https://doi.org/10.1076/ceyr.19.6.525.5283.
36. Kreger AS, Griffin OK. 1975. Cornea-damaging proteases of *Serratia marcescens*. Invest Ophthalmol 14:190–198.
37. Matsumoto K, Maeda H, Takata K, Kamata R, Okamura R. 1984. Purification and characterization of four proteases from a clinical isolate of *Serratia marcescens* kums 3958. J Bacteriol 157:225–232. https://doi.org/10.1128/JB.157.1.225-232.1984.
38. Schultz CL, Morck DW, McKay SG, Olson ME, Buret A. 1997. Lipopolysaccharide induced acute red eye and corneal ulcers. Exp Eye Res 64:3–9. https://doi.org/10.1006/exer.1996.0190.
39. Hume E, Sack R, Stapleton F, Willcox M. 2004. Induction of cytokines from polymorphonuclear leukocytes and epithelial cells by ocular isolates of *Serratia marcescens*. Ocul Immunol Inflamm 12:287–295. https://doi.org/10.1080/092739490500318.
40. Zhou R, Zhang R, Sun Y, Platt S, Szczotka-Flynn L, Pearlman E. 2012. Innate immune regulation of *Serratia marcescens*-induced corneal inflammation and infection. Invest Ophthalmol Vis Sci 53:7382–7388. https://doi.org/10.1167/iovs.12-10238.
41. Brothers KM, Stella NA, Romanowski EG, Kowalski RP, Shanks RM. 2015. EepR mediates secreted protein production, desiccation survival, and proliferation in a corneal infection model. Infect Immun 83:4373–4382. https://doi.org/10.1128/IAI.00466-15.
42. Cho CH, Lee SB. 2018. Comparison of clinical characteristics and antibiotic susceptibility between *Pseudomonas aeruginosa* and *P. putida* keratitis at a tertiary referral center: a retrospective study. BMC Ophthalmol 18:204. https://doi.org/10.1186/s12886-018-0882-3.
43. Konda N, Garg P, Sharma S, Willcox MDP. 2021. Risk factors for contact lens-related microbial keratitis and associated vision loss in a South Indian population. Eye Contact Lens 47:118–126. https://doi.org/10.1097/ICL.0000000000000737.
44. Porter AJ, Lee GA, Jun AS. 2018. Infectious crystalline keratopathy. Surv Ophthalmol 63:480–499. https://doi.org/10.1016/j.survophthal.2017.10.008.
45. Wang Q, Zhao Y, McClelland M, Harshey RM. 2007. The RcsCDB signaling system and swarming motility in *Salmonella enterica* serovar typhimurium: dual regulation of flagellar and SPI-2 virulence genes. J Bacteriol 189:8447–8457. https://doi.org/10.1128/JB.01198-07.
46. Morgenstein RM, Rather PN. 2012. Role of the Umo proteins and the Rcs phosphorelay in the swarming motility of the wild type and an O-antigen (*waaL*) mutant of *Proteus mirabilis*. J Bacteriol 194:669–676. https://doi.org/10.1128/JB.06047-11.
47. Norcross EW, Tullos NA, Taylor SD, Sanders ME, Marquart ME. 2010. Assessment of *Streptococcus pneumoniae* capsule in conjunctivitis and keratitis *in vivo* neuraminidase activity increases in nonencapsulated pneumococci following conjunctival infection. Curr Eye Res 35:787–798. https://doi.org/10.3109/02713683.2010.492462.
48. Reed JM, O'Callaghan RJ, Girgis DO, McCormick CC, Caballero AR, Marquart ME. 2005. Ocular virulence of capsule-deficient *Streptococcus pneumoniae* in a rabbit keratitis model. Invest Ophthalmol Vis Sci 46:604–608. https://doi.org/10.1167/iovs.04-0889.
49. Castelli ME, Vescovi EG. 2011. The Rcs signal transduction pathway is triggered by enterobacterial common antigen structure alterations in *Serratia marcescens*. J Bacteriol 193:63–74. https://doi.org/10.1128/JB.00839-10.
50. Lin CS, Horng JT, Yang CH, Tsai YH, Su LH, Wei CF, Chen CC, Hsieh SC, Lu CC, Lai HC. 2010. RssAB-FlhDC-ShlBA as a major pathogenesis pathway in *Serratia marcescens*. Infect Immun 78:4870–4881. https://doi.org/10.1128/IAI.00661-10.
51. Di Venanzio G, Stepanenko TM, Garcia Vescovi E. 2014. *Serratia marcescens* ShlA pore-forming toxin is responsible for early induction of autophagy in host cells and is transcriptionally regulated by RcsB. Infect Immun 82:3542–3554. https://doi.org/10.1128/IAI.01682-14.
52. O'Callaghan RJ, Callegan MC, Moreau JM, Green LC, Foster TJ, Hartford OM, Engel LS, Hill JM. 1997. Specific roles of alpha-toxin and beta-toxin during *Staphylococcus aureus* corneal infection. Infect Immun 65:1571–1578. https://doi.org/10.1128/IAI.65.5.1571-1578.1997.
53. Norcross EW, Sanders ME, Moore QC, III, Taylor SD, Tullos NA, Caston RR, Dixon SN, Nahm MH, Burton RL, Thompson H, McDaniel LS, Marquart ME. 2011. Active immunization with pneumolysin versus 23-valent polysaccharide vaccine for *Streptococcus pneumoniae* keratitis. Invest Ophthalmol Vis Sci 52:9232–9243. https://doi.org/10.1167/iovs.10-6968.
54. McDermott AM. 2013. Antimicrobial compounds in tears. Exp Eye Res 117:53–61. https://doi.org/10.1016/j.exer.2013.07.014.
55. Huang YH, Ferrieres L, Clarke DJ. 2006. The role of the Rcs phosphorelay in Enterobacteriaceae. Res Microbiol 157:206–212. https://doi.org/10.1016/j.resmic.2005.11.005.
56. Bertani G. 1951. Studies on lysogenesis. I. The mode of phage liberation by lysogenic *Escherichia coli*. J Bacteriol 62:293–300. https://doi.org/10.1128/JB.62.3.293-300.1951.
57. Barrick JE, Colburn G, Deatherage DE, Traverse CC, Strand MD, Borges JJ, Knoester DB, Reba A, Meyer AG. 2014. Identifying structural variation in haploid microbial genomes from short-read resequencing data using breseq. BMC Genomics 15:1039. https://doi.org/10.1186/1471-2164-15-1039.
58. Williams RN, Paterson CA, Eakins KE, Bhattacherjee P. 1982. Quantification of ocular inflammation: evaluation of polymorphonuclear leucocyte infiltration by measuring myeloperoxidase activity. Curr Eye Res 2:465–470. https://doi.org/10.3109/02713688208996350.
59. Khan S, Cole N, Hume EB, Garthwaite L, Conibear TC, Miles DH, Aliwaga Y, Krockenberger MB, Willcox MD. 2007. The role of CXC chemokine receptor 2 in *Pseudomonas aeruginosa* corneal infection. J Leukoc Biol 81:315–318. https://doi.org/10.1189/jlb.0506344.
60. Gipson IK, Spurr-Michaud S, Argüeso P, Tisdale A, Ng TF, Russo CL. 2003. Mucin gene expression in immortalized human corneal-limbal and conjunctival epithelial cell lines. Invest Ophthalmol Vis Sci 44:2496–2506. https://doi.org/10.1167/iovs.02-0851.
61. Kalivoda EJ, Stella NA, Aston MA, Fender JE, Thompson PP, Kowalski RP, Shanks RM. 2010. Cyclic AMP negatively regulates prodigiosin production by *Serratia marcescens*. Res Microbiol 161:158–167. https://doi.org/10.1016/j.resmic.2009.12.004.
62. Shanks RM, Kadouri DE, MacEachran DP, O'Toole GA. 2009. New yeast recombineering tools for bacteria. Plasmid 62:88–97. https://doi.org/10.1016/j.plasmid.2009.05.002.